Universal Journal of Physics and Application 9(6): 244-250, 2015 http://www.hrpub.org
DOI: 10.13189/ujpa.2015.090602

Study of the Mass Flow Rates on the Efficiency of Hybrid Thermal / Photvoltaique Sensor

Maifi Lyes[1,*], Kerbache Tahar[1] , Hioual Ouided[2]

[1]Physical Chemistry of Semi-Conductor Laboratory, University of Constantine, Algeria
[2] Department of Informatics, Faculty of Sciences & technology, University of Khenchela, Algeria

Abstract Hybrid thermal/photovoltaic systems associating a solar concentrator with a heat exchanger are an effective way to improve solar energy conversion yield. We present here an analysis of the effect of the mass flow rates in such a collector. A numerical simulation of the performance of the thermal/photovoltaic sensor with a heat exchanger including fins attached to the absorber and using air as a coolant is presented. A thorough analysis of the influence of the mass flow rate on the efficiency and the working of a thermal/photovoltaic collector is presented. The analysis is made using the equations of the components of heat transfer cascade into a matrix of four unknown's which are the glass , cells, fluid and insulation plate temperature. This matrix is solved by the fixed point method and Gauss-Seidel, at the permanent regime. Results show that the overall conversion efficiency of the system is increasing from 27% to 65%, and the cell temperatures decreasing from 345°K to 335°K when mass flow rates varies from 0.02 kg/s to 0.1 kg/s.

Keywords Thermal Photovoltaic, Cells Solar, Parabolic-concentrator, Permanent Regime, Heat Exchanger

1. Introduction

Problems of environmental pollution and energy lack in the world have become much serious recently. Solar energy as a renewable and environmentally friendly energy has the potential to meet global energy demand in the future. Methods for the conversion of solar energy can be classified into two types: a thermal option, that converts solar energy into heat, subsequently transformed into electricity, and the photovoltaic methods that converts solar energy directly into electrical energy. Usually, these two methods, while perfectly compatible, are used separately leading to a low efficiency. In order to improve conversion yield, a new solar thermal combined system, has been developed to harness heat and electricity simultaneously. In 1978, kern and all [1] presented a prototype of a thermal/photovoltaic system using air and water as a coolant to reduce the temperature of the solar cells. A number of theoretical and experimental studies to assess the efficiency of hybrid thermal/photovoltaic system have been performed [2-7]. Florschuetz and all [2] used the model of hotel-Whillier to analyze the performance of the hybrid solar system that could provide domestic hot water. Garg and all [3] have developed a stable model to simulate the performance of thermal/photovoltaic hybrid system. In the recent years much research has been reported in the literature on new solar thermal systems with lower costs [4-7]. When sunlight is concentrated on the solar cell, most of the energy absorbed by the cell is converted into thermal energy which in turn increases the temperature and reduces the electrical efficiency. Therefore, it is necessary to remove heat from the cell by a heat transfer fluid (air, water…).

2. System Model

The system model consists of two part: the first calculates the thermal heat system parameters such as temperature (T), thermal energy (Q) and thermal efficiency (η_{th}) of the sensor, and the second part is devoted to the electrical model, which calculates the current (I), voltage (V) and the generated electric power. The hybrid thermal/photovoltaic collector considered in this work is shown in (figure 1). The glass cover (in plastic) is inserted in order protect the sensor against mechanical damage, the light is reflected and concentrated on the solar cell by a reflective cylindro-parabolic concentrator. The focusing system consists of the cylindro-parabolic concentrators. Each one has seven panels from (Generic 60 WP polycrystalline), with 36 cells in series for each panel. The panels are connected in series along the direction of the system; they are glued and sealed to keep surfaces cells clean. Fins are fixed on the heat exchanger to improve heat exchanger bottom the fluid and the solar cells. The heat exchanger bottom is covered with a good insulator to minimize heat losses to the ambient [7].

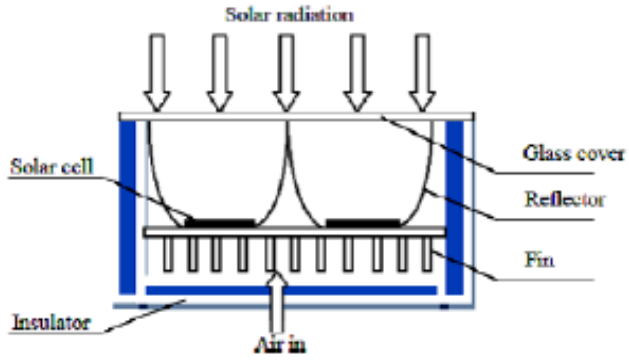

Figure 1. Schematic view of our thermal/photovoltaic sensor

2.1. Thermal Model

(Figure 2) shows the thermal model of the system. For the sake of simplicity, the following hypotheses are made

- A one-dimensional steady state heat transfer in the direction of the flow.
- The heat capacities of the glass, concentrator, solar cell, fins, absorber and the insulating plate are negligible.
- The parabolic concentrator is ideal and all the incident radiation in the acceptance angle can reach the solar cells.
- The solar radiation converted into thermal energy is completely absorbed by the panels and solar absorber.
- The temperature of the solar cell and the absorber are uniform.

Based on these assumptions, the equations of energy can be written as follows:

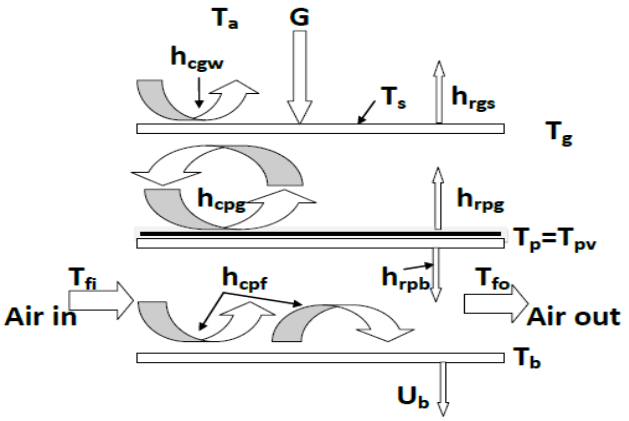

Figure 2. Thermal model of our thermal/photovoltaic sensor

Where:

h_{cgw} Convective heat transfer between glass/ambient.

h_{cpg} heat transfer by natural convection between glass/ cells solar.

h_{cpf} heat transfer by forced convection between fluid, insulating plate and absorber.

h_{rgs} heat transfer by radiation between glass/ambient.

h_{rpg} heat transfer by radiation between glass/cells solar.

h_{rpb} heat transfer by radiation between absorber/insulating plate.

T_a ambient temperature.

T_s ceil temperature .

T_g ,T_P ,T_{pv} ,T_b, T_f are temperatures glass, absorber, cells solar, insulating plate and fluid respectively.

T_{fi} and T_{fo} are fluid temperatures in and out respectively.

2.1.1. For the glass cover

$$\alpha_g GC\left(1+\tau_g\rho_g\rho_R^{2n}\right)=h_{rgs}\left(T_g-T_s\right)+h_{cgw}\left(T_g-T_w\right)+h_{cpg}\left(T_g-T_p\right)+\frac{A_{ct}}{A_c}h_{rpg}\left(T_g-T_p\right) \quad (1)$$

Where n is the average number of reflection for radiation inside the acceptance angle, where A_{ct}, A_{cb} and A_c are the areas (m^2) of reflector, solar cell and convection, respectively, G is solar irradiation ($W.m^{-2}$) and C the concentrating ratio is 2.

2.1.2. At the thermal/photovoltaic plate

$$\tau_g\alpha_p G\rho_R^n d\left(1+\frac{\rho_p\rho_g\rho_R^{2n}}{C}\right)(1-P)+\tau_g\alpha_p GP\rho_R^n d\left(1+\frac{\rho_{pv}\rho_g\rho_R^{2n}}{C}\right)\left(1-\eta_{pv}\right)=\frac{A_{cb}}{A_c}h_{cpf}\eta_p\left(T_p-T_f\right)+\frac{A_{cb}}{A_c}h_{rpb}\left(T_p-T_b\right)+\frac{A_{ct}}{A_c}h_{cpg}\left(T_P-T_f\right)+\frac{A_{ct}}{A_c}h_{rpg}\left(T_p-T_g\right) \quad (2)$$

The solar reflectivity of the glass cover ρ_g , of the photovoltaic cell surface ρ_{pv} and of plate ρ_p are assumed to be the same as that of black absorber ($\rho_g=\rho_p=\rho_{pv}$). Where d is a correction for the gap loss. The value of the glass transmittance τ_g is 0.9, and plate absorptivity α_p, and glass absorptivity α_g are 0.9 and 0.06, respectively [8,9,10] .

2.1.3. The heat exchanger

$$\frac{m_p C_f}{w}\frac{dT_f}{dx}=h_{cpf}\left(T_b-T_f\right)+\frac{A_{cb}}{A_c}h_{cpf}\eta_p\left(T_p-T_f\right) \quad (3)$$

Where m_p is mass flow rate ($kg.s^{-1}$), C_f is specific heat ($J.kg^{-1}.k^{-1}$) and w is system width (m) [11,12].

2.1.4. The insulating plate

$$U_b\left(T_b-T_a\right)=h_{cpf}\left(T_f-T_b\right)+\frac{A_{cb}}{A_c}h_{rpb}\left(T_p-T_b\right) \quad (4)$$

The back loss coefficient U_b is 0.0692 $W.m^2.k$ [12].

2.2. Electrical Model

The semiconductors p-n junction and a current source (photocurrent) which mimics the electrical energy obtained from the light flux. Losses arising from junction leakage, contacts and connections resistance are taken into account by shunt (R_{sh}) and series (R_s) resistances. The model commonly used for a solar cell or a photovoltaic module in an electrical circuit is sketched in (figure 3). To enable comparisons, the manufacturers give either the I versus V or E_{pv} versus V curves depending on lighting and temperature, or typical operating values (I,V) corresponding to short circuit (I_{cc} ,0), open circuit (0, V_{oc}), and maximal power

(I,V). These three pairs of values were measured under standard test conditions illumination G_{ref}=1000 W.m^{-2}, temperature T_{jref}=25°C.

$$I = I_{ph} - \frac{V+R_sI}{R_{sh}} - I_0\left(\exp\left(\frac{q_i(V+R_sI)}{n_s\gamma KT_j}\right) - 1\right) \quad (5)$$

$$I_{ph} = I_{ccref}\, G/G_{ref} + c_t(T_J - T_{jref}) \quad (6)$$

$$I_0 = I_{0ref}\left(\frac{T_J}{T_{jref}}\right)^3 \exp^{\left(\frac{q_iE_g}{n_s\gamma K}\right)\left(\frac{1}{T_{jref}}\right)-\left(\frac{1}{T_J}\right)} \quad (7)$$

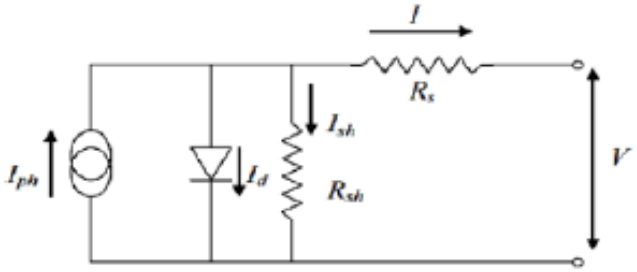

Figure 3. Electrical model of our sensor thermal/ photovoltaic

Where I_{Ph}, I_{ccref} and I_0 is the photocurrent, reference current of short-circuit and the saturation diode current (in A) respectively, T_j is the junction temperature of the cells (°K) and q_i is the charge of the electron, K is the Boltzmann constant, E_g is the gap energy (eV), γ is the ideality factor of the junction with values between 1-2 and I_{Oref} is a coefficient dependent on temperature and on the cell technology [14]. G is the illumination (W.m^{-2}), I_{cc} is the short-circuit current (A) and c_t is the temperature coefficient of the short-circuit current (A.K^{-1}) given by the manufacturer. Following equation (5), it is easy to assume that the current intensity is mainly proportional to the lighting, whereas the other parameters (E_g,I_{cc},R_{sh},R_s and γ) vary strongly with the temperature and the technology used [15].

3. Method of Calculation

We can write the equation 3 as:

$$\frac{dT_f(x)}{dx} + pT_f(x) = q \quad (8)$$

Where p and q are constants obtained by algebraic manipulations.

The boundary conditions are :

$$T_f(x) = T_a, \text{at } x = 0$$

$$T_f(x) = T_0, \text{at } x = L$$

The solution can be obtained as

$$T_f(x) = \frac{q}{p} + \left(T_a - \frac{q}{p}\right)\exp^{-px} \quad (9)$$

By grouping the four equations from equation 1 to equation 4, we obtain a four variables matrix. In the equation 9, p and q are the two unknown temperatures functions. An iterative algorithm is applied to determine these temperatures. In order to calculate the temperature of each cell of the photovoltaic concentrator, the panels is divided into n=252 units of 0.031746 m length (n is also the number of series cells in the collector). To stsrt the calculation, initial values at T_g,(T_p=T_{pv}) and T_b are introduced. The temperature T_f of the in air flow at x=0, is equal to the ambient temperature. The new temperatures can be obtained from the matrix. Gauss-seidel method is used to calculate the temperatures of each cell by an iterative process which is repeated until temperature values converge. Thus the components temperatures for the first cell can be determined. Applying it as the intel to the next cell, the components temperatures for the second cell can be similarly calculated. By repeating this step, all temperatures for the different components can be determined. Using these temperatures, one can deduce the air mass flow influence on the cells and panel efficiency.

4. Performance Parameters

Performance parameters of the hybrid sensor thermal/photovoltaic are computed as following:

The thermal energy gained by the air flow through the system of thermal/photovoltaic is:

$$Q = \sum_{j=1}^{n} m_p \,.\, C_f \,.\, (T_{0,j} - T_{i,j}) \quad (10)$$

The thermal efficiency of the system is:

$$\eta_{th} = \frac{\sum_{j=1}^{n} m_p C_f (T_{o,j} - T_{i,j})}{GC} \quad (11)$$

The electric power produced by the system is [15].

$$E_{pv} = I.V \quad (12)$$

The electrical efficiency of the system is:

$$\eta_{pv} = \frac{IV}{GC} \quad (13)$$

The combined thermal/photovoltaic efficiency is the sum of photovoltaic and thermal efficiencies of the system.

$$\eta_{tot} = \eta_{pv} + \eta_t \quad (14)$$

5. Results and Discussion

Thermo-physical and internal, used in the calculation are shows in (table 1). The dimension of the system is (w=2m x L= 7.8 m). the dimensions of the fins are (δ=0.0015m x H=0.025 x L=7.8m). Panel dimensions (w_p=1.189m x L_p=0.595m). the values of the radiation G and the ambient temperature T_a used in this study are constants in a calculation.

Table 1. Thermo-physical and internal parameters of the system photovoltaic panels

Paramètre	value	Paramètre	value
α_g	0.04	U_b	0.5 $W.m^{-2}.°k^{-1}$
G	800 $W.m^{-2}$	ε_g	0.86
C	2	σ	$5.6697.10^{-8}$ $W.m^{-2}.°k^{-4}$
τ_g	0.90	ε_b	0.95
ρ_g	0.06	ε_p	0.95
ρ_R	0.94	R_{sh}	300 Ω
n	0.61	I_{ph}	3.8 A
d	0.95	C_f	1008 $J.Kg^{-1}.°K^{-1}$
ρ_p	0.05		
ε_{pv}	0.95		
P	0.52		
α_p	0.95		
α_{pv}	0.90		
ρ_{pv}	0.05		

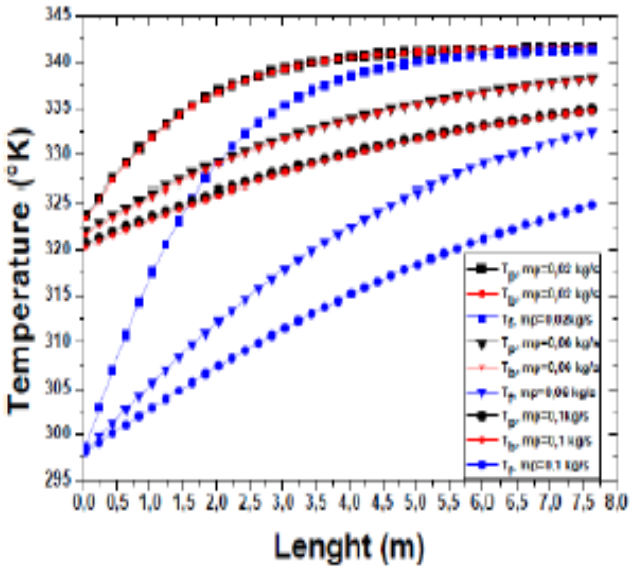

Figure 4. The mass flow influence on the fluid, cells and insulating plate temperature

Figure 4 shows the effects of the mass flow rate on the temperature of the fluid, the cells and insulating plate respectively as a function of the position along the panel length. It can be observed that all the temperature, increase with the position. Increasing of the air mass flow rate will decrease the temperature of the system, at constant sunlight radiance. This is explained by the fact by the increase of air amount at a given heat load, leading to a reduction of its temperature of exit.

Figure 5. The mass flow influence on the thermal efficiency

The figure 5 and figure 6, show the effect of the mass flow on thermal and electrical efficiency of the system respectively in the air flow direction. The efficiency thermal and electrical increases with the air flow direction, the electric efficiency increase is linear and we have a small increase in the curves when the mass flow increases in the range higher than 3m along the air flow direction. The thermal efficiency increases in exponential in the air flow direction, and is very important when the mass flow increases figure 5. This is due to the improvement in internal convective exchangers at a constant heat loss when the air flow increases. The thermal conversion efficiency of the system is increasing from 18% to 55%, when a mass flow rate varies from 0.02 kg/s to 0.1 kg/s.

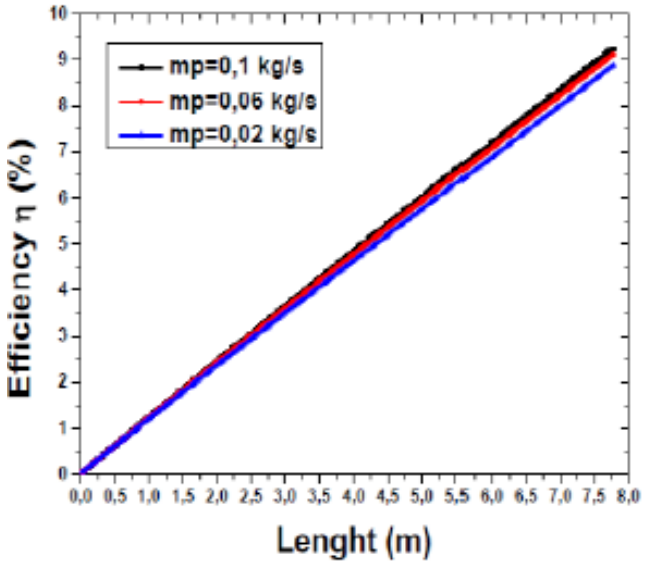

Figure 6. The mass flow influence on the electric efficiency

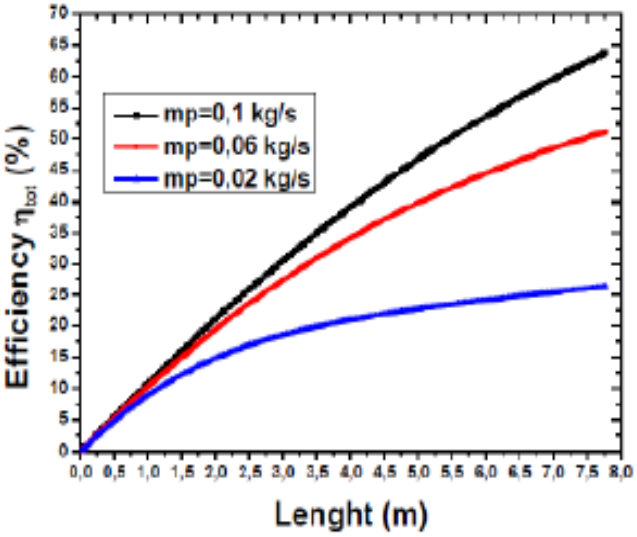

Figure 7. The mass flow influence on the total efficiency

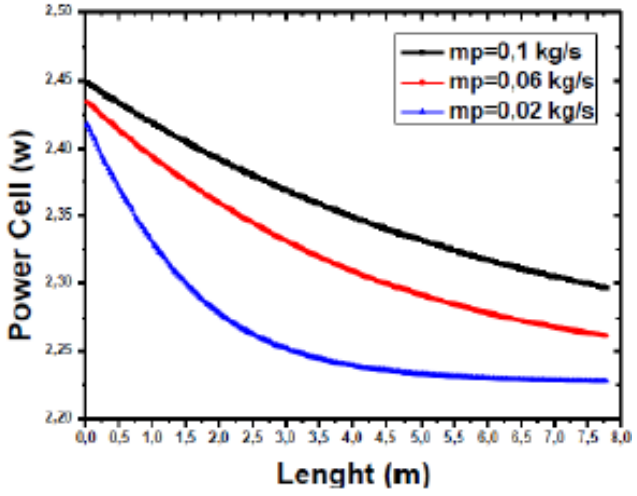

Figure 8. The mass flow influence on the electric power of each cell

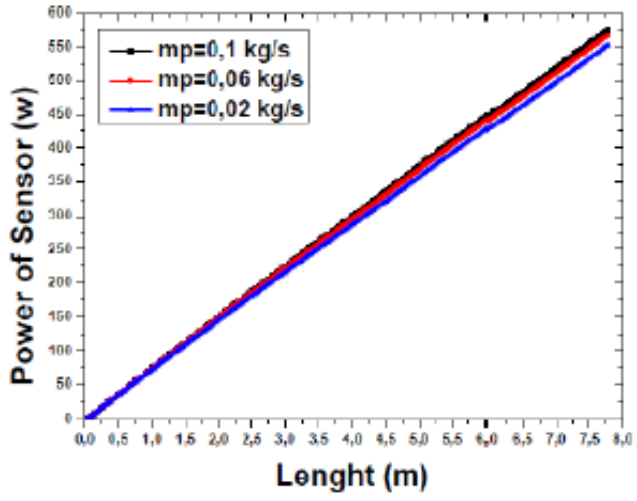

Figure 9. The mass flow influence on the electric power of sensor

The figure 7 to 9 show the mass flow rate influence on the cumulative efficiency the electric power of each cell and electric power of the sensor in the air flow direction respectively. The curve of the power electric of sensor is identical in a length smaller than 3m but above 3m there is small increase when the mass flow is increasing, and the difference in the total efficiency is important with the increasing of the mass flow. This trend is explained by the fact that when the mass flow increases, the cells are cooled which increases the electric power and the total efficiency. Note that the power of each cell decreases in the air flow direction when the temperature increases, but for a given point in the sensor length this value increases because the mass flow rate increases. the total conversion efficiency of the system is increasing from 27% to 65%, when mass flow rates varies from 0.02 kg/s to 0.1 kg/s.

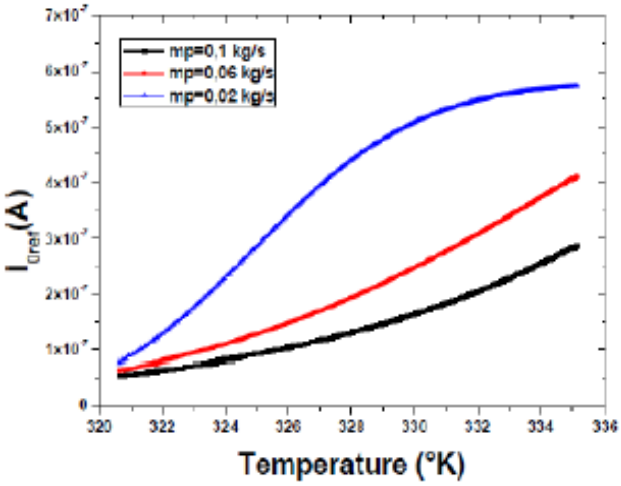

Figure 10. The variation of the reference current according in the cell temperatureell

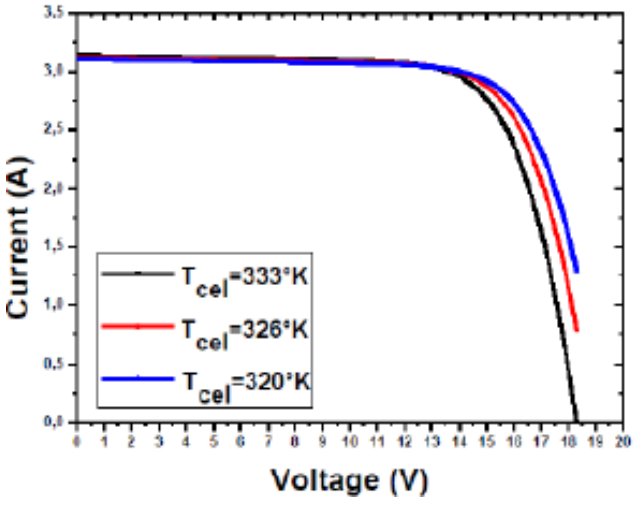

Figure 11. The variation of the panel current according on the panel voltage

The variation of the reference current as a function of the cell temperature is shown in the figure 10. The reference current increase, with the increase of the cell temperature, the losses by effect of joule, increases, therefore the each cell electric power decreases. In the same figure if the mass

flow increases, the reference current at a given position, decreases. This is induced from the fact that the increase of the mass flow rate strongly cools the cells. If we consider figure 11, we deserve the current decreasing when the temperature increases. This is consistent with the physical principles governing cells behavior. Indeed, the current (I) is proportional to the mobility and the density of electrons and holes. To the density of these carrier's is constant in the used temperature domain, the current at constant, voltage is proportional to the carrier's mobility. It is known that the carrier's mobility decreases when the temperature increases. This is due to the strong diffusion of the charge carrier's by, the crystalline lattice and localized on doping atoms photons. This diffusion decreases the carrier's mobility, so the electric current, which is in agreement with our results.

7. Conclusions

Using our model, we have shown, the amount of heated air rises with the air mass flow rate increases. This causes a decrease in the outlet temperature which then cools, the solar panel, owing to an improvement in the internal convective heat transfer. Consequently, the thermal and the electrical performance of the system is enhanced. The increase of the electrical efficiency for solar cells following the decrease in their temperature has a beneficial effect on the electrons and holes mobility. This carrier mobility increases as the temperature decreases. The results obtained suggest that it is a good alternative to conventional photovoltaic systems. Extracted heat could be used for heating the air or be transformed into another energy or help prevent the problem of (hot spots) in photovoltaic generators.

Appendix

ηp is the total efficiency of the absorber plate [9].

$$\eta_p = \frac{A_c + A_{fin}\eta_{fin}}{A_{cb}} \quad (13)$$

And η_{fin} is fin efficiency defined as:

$$\eta_{fin} = \frac{\tanh(\omega H_{fin})}{\omega H_{fin}} \quad \text{And} \quad \omega = \frac{2h_{cpf}}{\lambda_{fin}\delta_{fin}} \quad (14)$$

The convective heat transfer coefficients, h_{cpf} is calculated using the following relationship [10].

$$h_{cpf} = \left(\frac{\lambda_f}{D}\right)(0.0158R_e^{0.8} + (0.00181R_e + 2.92)\exp^{-\frac{0.03795X}{D}} \quad (15)$$

The convection heat transfer coefficient between the solar cells and the glass cover is calculated from the relation [11]:

$$h_{cpg} = \left(\frac{\lambda_f}{H_{pg}}\right)\left(1 + 1.44\left(1 - \frac{1708}{R_a\cos\beta}\right)\left(1 - \frac{\sin(1.8\beta)^{1.6}1708}{R_a\cos\beta}\right) + (R_a\cos\beta/5830)^{\frac{1}{3}} - 1\right) \quad (16)$$

Where Re and Ra are Reynolds and Rayleigh numbers respectively [11] and convective losses due to the wind is assumed to be 25 W/m2. K. All other radiative heat transfer coefficients are taken as 6 W/m2.K.

In equation 6, p and q are the temperature functions for various components of the hybrid thermal/photovoltaic system.

Where

$$p = h_{cpf}\left(\frac{A_{cb}}{A_c}\eta_p + 1\right)/\left(\frac{m_p C_f}{w}\right) \quad (17)$$

And

$$q = \frac{\frac{A_{cb}}{A_c}h_{cpf}\eta_p T_p + h_{cpf}T_b}{\frac{m_p C_f}{w}} \quad (18)$$

REFERENCES

[1] Kern Jr E C, Russell M C. Combined photovoltaic and thermal hybrid collector system. In: Proceedings of 13th IEEE Photovoltaic Specialist, 1978. 1153—1157.

[2] L.W. Florschuetz, Extension of the Hottel-Whillier model to the analysis of combined photovoltaic thermal flat collector, Sol. Energy. 22 (1979) 361-366.

[3] H.P. Garg, R.S Adhikari, Conventional hybrid photovoltaic thermal (PV/T) air heating collectors: Steady-state simulation, Renewable Energy. 11 (1997) 363-385.

[4] H.P. Garg and R.S. Adhikari, Performance analysis of a hybrid photovoltaic/thermal (PV/T) collector with integrated CPC troughs, Int. J. Energy. Res. 23 (1999) 1295-1304.

[5] G.R. Whitfield, R.W. Bentley, C.K. Weatherby, B. Clive, The development of small concentrating pv systems, Proc. of 29th IEEE PVSC. New Orleans. (2002) 1377-1379.

[6] M.Y. Othman, B. Yatim, Performance analysis of a double-pass photovoltaic/thermal (PV/T) solar collector with CPC and fins, Renewable Energy. 30 (2005) 2005-2017.

[7] X. Chen, Y.M. Xuan, Y.G. Han, Investigation on performance of a solar thermophotovoltaic system, Sci. China. Ser. E-Tech. Sci. 51 (2008) 2285-2294.

[8] R. Ari, Optical and thermal properties of compound parabolic concentrators, Sol. Energy. 18 (1976) 497-511.

[9] K. Sopiana, H.T. Liu, S. Kakac, T.N. Veziroglu, Performance of a double pass photovoltaic thermal solar collector suitable for solar drying systems, Ener. Conv. Manage. 41 (2000) 353-365.

[10] S. Sharples, P.S. Charlesworth, Full-scale measurements of wind- induced convective heat transfer from a roof-mounted flat-plate solar collector, Sol. Energy. 62 (1998) 69-77.

[11] S.J. Anand, T. Arvind, Energy and exergy efficiencies of a hybrid photovoltaic–thermal (PV/T) air collecto, Renewable Energy. 32 (2007) 2223-2241.

[12] A. Duffine, W.A. Beckman, Solar Engineering of Thermal Processes, John Wiley & Sons, New York, 1991.

[13] G. Walker, Evaluating MPPT converter topologies using a

MATLAB PV model, J. Electr. Electron. Eng. 21 (2001) 49–56.

[14] R. Kadri, H. Andrei, J. P. Gaubert, T. Ivanovici, G. Champenois, P. Andrei, Modeling of the Photovoltaic Cell Circuit Parameters for Optimum Connection Model and Real-Time Emulator with Partial Shadow Conditions, Energy. 42 (2012).

[15] Ramos Hernanz, JA., Campayo Martín, J.J., Zamora Belver, I., Larrañaga Lesaka, J.,Zulueta Guerrero, E., Puelles Pérez, E, Modelling of Photovoltaic Module, Conference on Renewable Energies and Power Quality (ICREPQ'10) Granada (Spain), March,2010.